Static quark anti-quark interactions at zero and finite temperature QCD.
II. Quark anti-quark internal energy and entropy

Olaf Kaczmarek*

Fakultät für Physik, Universität Bielefeld, D-33615 Bielefeld, Germany

Felix Zantow†

Physics Department, Brookhaven Natl. Laboratory, Upton, New York 11973, USA

(Dated: May 1, 2019)

We analyze the change in free energy, internal energy and entropy due to the presence of a heavy quark anti-quark pair in a QCD heat bath. The internal energies and entropies are introduced as intensive observables calculated through thermal derivatives of the QCD partition function containing additional static color sources. The quark anti-quark internal energy and, in particular, the entropy clearly signal the phase change from quark confinement below and deconfinement above the transition and both observables are introduced such that they survive the continuum limit. The intermediate and large distance behavior of the energies reflect string breaking and color screening phenomena. This is used to characterize the energies which are needed to dissolve heavy quarkonium states in a thermal medium. Our discussion supports recent findings which suggest that parts of the quarkonium systems may survive the phase transition and dissolve only at higher temperatures.

PACS numbers: 11.15.Ha, 11.10.Wx, 12.38.Mh, 25.75.Nq

I. INTRODUCTION

This is the second part of our discussion of thermal modifications of the strong forces in finite temperature QCD [1] (for a detailed introduction to this subject and further references see [1, 2]). At finite temperature, $T \neq 0$, the free energy of a static quark anti-quark pair [3, 4], separated by distance r, is an important tool to analyze the in-medium modification of the QCD forces. Similar to the free energies also the internal energies have recently been introduced [5, 6] and are expected to play an important role in the discussion of quarkonia binding properties [7, 8, 9, 10, 11, 12, 13, 14, 15, 16, 17]. Moreover, the structure of these energies at large distances and high temperatures is important for our understanding of the bulk properties of the QCD plasma phase, *e.g.* the screening property of the quark gluon plasma [18, 19], the equation of state [20, 21]. They also provide important input to the construction of effective models based on properties of the Polyakov loop [1, 5, 22, 23, 24, 25]. Up to quite recently [1, 21, 23, 26, 27, 28] most of these discussions concerned the quark anti-quark free energies in quenched QCD. Several qualitative differences, however, are to be expected when changing from free to internal energies and/or when taking into account the influence of dynamical fermions. The difference between free and internal energy arises from non-trivial entropy contributions [5, 6]. Moreover, in QCD with light dynamic quarks the large distance behavior of the strong interaction will show a qualitative different behavior due to the possibility of string breaking.

Properties of the finite temperature quark anti-quark free energies and the heavy quark potential at $T = 0$, $V(r)$, have been discussed for 2-flavor QCD in Refs. [1, 21, 23, 27, 28]. Recently some results have also been reported for 3-flavor QCD [26]. Here we will continue our analysis of the fundamental forces of QCD at finite temperature. We analyze the partition function of 2-flavor QCD in the presence of heavy quarks and extract the quark anti-quark internal energies and entropies. This paper is organized as follows: In section II we introduce the change in internal energy and entropy due to the presence of static quarks and anti-quarks in a thermal heat bath. We discuss their temperature dependence at large distances, in particular, their behavior in the vicinity of the transition, in section III. We finally discuss the qualitative and quantitative differences between free and internal energies in section IV and discuss their binding properties with respect to quarkonium binding in the vicinity of the transition. Section V contains our conclusions. Details on our simulation parameters, the lattice actions used in our calculations as well as details on the analysis of the quark anti-quark free energies are given in Ref. [1].

II. PARTITION FUNCTION IN THE PRESENCE OF HEAVY QUARKS

A. Free energy, internal energy and entropy

As we are interested in the lattice formulation of QCD at finite temperature in thermal equilibrium, we consider the (Euclidean) path integral, *i.e.* we consider the partition function of the QCD heat bath,

$$\mathcal{Z}(T,V) \equiv \int dA d\Psi d\bar{\Psi} e^{-S[A,\Psi,\bar{\Psi}]} = e^{-F(T,V)/T}, \quad (1)$$

*Electronic address: okacz@physik.uni-bielefeld.de
†Electronic address: zantow@quark.phy.bnl.gov

where T (V) denotes the temperature (volume) and $S[A, \Psi, \bar{\Psi}]$ the QCD action. We also investigate the corresponding system containing additional heavy quarks [3], *i.e.*

$$\mathcal{Z}_{\mathcal{O}}(r, T, V) \equiv \int dA d\Psi d\bar{\Psi} \; \mathcal{O}_r^{(c)}[W, W^\dagger] \; e^{-S[A, \Psi, \bar{\Psi}]}$$
$$= e^{-\tilde{F}_{\mathcal{O}}(r, T, V)/T} \;, \qquad (2)$$

where $\mathcal{O}_r^{(c)}[W, W^\dagger]$ denotes an operator which introduces static color sources representing quarks and anti-quarks separated by distances $r \equiv \{r_i\}$ in a specific color representation c. A static color source appearing in $\mathcal{O}_r^{(c)}[W, W^\dagger]$ located at $\mathbf{x}$ is described by the thermal Wilson line,

$$W(\mathbf{x}) = \mathcal{T} \exp \left(i \int_0^{1/T} dx_0 \; \lambda \cdot \mathbf{A}_0(x_0, \mathbf{x}) \right) \;. \quad (3)$$

The expectation value of $\mathcal{O}_r^{(c)}[W, W^\dagger]$, *i.e.* the n-point Polyakov loop correlation function $\langle \mathcal{O}_r^{(c)}[W, W^\dagger] \rangle$, is related to the change in free energy, $F_{\mathcal{O}}(r, T) \equiv \tilde{F}(r, T, V) - F(T, V)$, due to the presence of static quark anti-quark sources in the heat bath,

$$F_{\mathcal{O}}(r, T) = -T \ln \langle \mathcal{O}_r^{(c)}[W, W^\dagger] \rangle + T C_{\mathcal{O}} \qquad (4)$$
$$= -T \left(\ln \mathcal{Z}_{\mathcal{O}}(r, T, V) - \ln \mathcal{Z}(T, V) \right) + T C_{\mathcal{O}} \;,$$

where $C_{\mathcal{O}}$ can be fixed through renormalization [29]. For instance, in the case of 2-point Polyakov loop correlation

functions the singlet (1), averaged ($\bar{q}q$) and octet (8) color representations of the operator $\mathcal{O}_r^{(c)}[W, W^\dagger]$ can be specified as [3, 30, 31]

$$\mathcal{O}_r^{(1)}[W, W^\dagger] = \frac{1}{3} \mathrm{Tr} \; W(0) \; W^\dagger(|r|) \;, \qquad (5)$$

$$\mathcal{O}_r^{(\bar{q}q)}[W, W^\dagger] = \frac{1}{9} \mathrm{Tr} \; W(0) \; \mathrm{Tr} \; W^\dagger(|r|) \;, \qquad (6)$$

$$\mathcal{O}_r^{(8)}[W, W^\dagger] = \frac{1}{8} \mathrm{Tr} \; W(0) \; \mathrm{Tr} \; W^\dagger(|r|)$$
$$- \frac{1}{24} \mathrm{Tr} \; W(0) \; W^\dagger(|r|) \;. \qquad (7)$$

The color singlet, averaged and octet quark anti-quark free energies, *i.e.* $F_1(r, T)$, $F_{\bar{q}q}(r, T)$ and $F_8(r, T)$, respectively, have already been discussed extensively in quenched and full QCD [1, 5, 19, 23, 26, 27, 28, 32, 33, 34].

For the purpose of discussing internal energies ($U_{\mathcal{O}}(r, T)$) and entropies ($S_{\mathcal{O}}(r, T)$), we follow the conceptual approach suggested in Refs. [5, 6] and consider thermal derivatives of the QCD partition functions introduced above, *i.e.*

$$U_{\mathcal{O}}(r, T) = -T^2 \frac{\partial F_{\mathcal{O}}(r, T)/T}{\partial T} \;, \qquad (8)$$

which leads to

$$U_{\mathcal{O}}(r, T) = -T^2 \left(\frac{1}{\langle \mathcal{O}_r^{(c)}[W, W^\dagger] \rangle} \langle \mathcal{O}_r^{(c)}[W, W^\dagger] \frac{\partial S[A, \Psi, \bar{\Psi}]}{\partial T} \rangle - \langle \frac{\partial S[A, \Psi, \bar{\Psi}]}{\partial T} \rangle \right)$$
$$\equiv \tilde{U}_{\mathcal{O}}(r, T, V) - U(T, V) \;. \qquad (9)$$

Note here that the derivative of the operator $\mathcal{O}_r^{(c)}$ with respect to temperature, $\partial \mathcal{O}_r^{(c)}/\partial T$, vanishes due to (3). A similar relation can be derived for the entropies starting from

$$S_{\mathcal{O}}(r, T) = -\frac{\partial F_{\mathcal{O}}(r, T)}{\partial T}$$
$$\equiv \tilde{S}_{\mathcal{O}}(r, T, V) - S(T, V) - \frac{\partial T C_{\mathcal{O}}}{\partial T} \;, (10)$$

i.e. the observable $T S_{\mathcal{O}}(r, T)$ could be calculated from the difference, $T S_{\mathcal{O}}(r, T) = U_{\mathcal{O}}(r, T) - F_{\mathcal{O}}(r, T)$, with $U_{\mathcal{O}}(r, T)$ and $F_{\mathcal{O}}(r, T)$ given in (9) and (4). We have also specified constant contributions, $C_{\mathcal{O}}$, which result from divergent contributions to the free energies and will control the internal energies and entropies at large quark anti-quark separations. Once the free energies are fixed

through renormalization also the constant contributions to the internal energies and entropies are properly determined.

We note that Eq. (9), and similar (10), open the possibility for a direct calculations of $U_{\mathcal{O}}(r, T)$ and $S_{\mathcal{O}}(r, T)$ and define properly the quantities we aim to discuss here, *i.e.* the change in internal energies and entropies due to the presence of static quarks and anti-quarks in the QCD heat bath. Quite similar to the change in free energies, $F_{\mathcal{O}}(r, T) = \tilde{F}_{\mathcal{O}}(r, T) - F(T)$, also the changes in internal energies and entropies, $U_{\mathcal{O}}(r, T) = \tilde{U}_{\mathcal{O}}(r, T, V) - U(T, V)$ and $S_{\mathcal{O}}(r, T) = \tilde{S}_{\mathcal{O}}(r, T, V) - S(T, V)$, are expected to behave like intensive observables and, in particular, will show no volume dependence in the thermodynamic limit. It, however, can no longer be assumed that the r-dependence of the quark anti-quark free energies (4) are

given by the r-dependences of the internal energies (9) alone, *i.e.* we expect

$$F_{\mathcal{O}}(r,T) = U_{\mathcal{O}}(r,T) - TS_{\mathcal{O}}(r,T) . \qquad (11)$$

This indicates a quite complicated relation between free energies, internal energies and entropies and stresses the important role of the entropy contribution which is still present in free energies. In the limit of vanishing temperature, $T \to 0$, however, $TS_{\mathcal{O}}(r,T \to 0)$ will vanish and

$$F_{\mathcal{O}}(r,T \equiv 0) = U_{\mathcal{O}}(r,T \equiv 0) \equiv V_{\mathcal{O}}(r) , \qquad (12)$$

i.e. $F_{\mathcal{O}}(r,T \to 0)$ and $U_{\mathcal{O}}(r,T \to 0)$ could be used[1] to define the corresponding energies at $T = 0$.

Unfortunately, the non-perturbative formulation of energies given in (9) is still complicated and, in particular, it is complicated to be given in a form suitable for lattice simulations [21, 35, 36, 37]. In the thermodynamic limit, however, the internal energy and entropy described above can be calculated equally well from Eqs. (8, 10). We indeed have used these relations and performed the derivatives with respect to temperature based on finite difference approximations using the non-perturbative free energies at neighboring temperature as input (see Tab. 1 of Ref. [1]). With this method no perturbative uncertainties get introduced in our calculations and a test of confinement and deconfinement could be given. In fact, as we use in our calculations the renormalized free energy as input, both quantities, the internal energies and entropies, survive the continuum limit. We stress here, however, that we also provide non-perturbative renormalization prescriptions for the quark anti-quark internal energies and entropies which are independent from a renormalization of the quark anti-quark free energies.

B. Theoretic expectations and renormalization

Following [1] we consider mainly the quark anti-quark internal energies and entropies in the color singlet channel. At large distances and high temperatures, *i.e.* $rT \gg 1$, T sufficiently above T_c, as well as at small distances and zero temperature, *i.e.* $r\Lambda_{\mathrm{QCD}} \ll 1$, the singlet free energies, $F_1(r,T)$, are indeed dominated by one gluon exchange [1]. Using the perturbative small distance relation for the singlet free energy [3, 30, 38, 39],

$$F_1(r,T) \simeq -\frac{4}{3}\frac{\alpha(r)}{r} \quad , \ r\Lambda_{\mathrm{QCD}} \ll 1 , \qquad (13)$$

standard thermodynamic relations (Eqs. (8) and (10)) lead to

$$U_1(r \ll 1/\Lambda_{\mathrm{QCD}},T) \simeq -\frac{4}{3}\frac{\alpha(r)}{r} , \qquad (14)$$

and

$$S_1(r \ll 1/\Lambda_{\mathrm{QCD}},T) \simeq 0 . \qquad (15)$$

We thus expect that at small distances the singlet free and internal energies are controlled to a large extent by energy, *i.e.* in the limit of small distances both will smoothly approach the zero temperature heavy quark potential, $V(r)$. At larger distances, however, the quark anti-quark free energies are strongly temperature dependent [1, 27, 28] and thus non-vanishing entropy contributions arise. In this case differences between free and internal energies are expected to become important and the quark anti-quark free energy will be to a large extent controlled by $TS_1(r,T)$.

To clarify the role of the entropy we compare[2] in Fig. 1(a) the short and large distance parts of the singlet free and internal energies at $T \simeq 1.3T_c$ and show in Fig. 1(b) the corresponding entropy contribution, $TS_1(r,T \simeq 1.3T_c)$. We also indicate in both figures the small distance behavior expected from Eqs. (14) and (15) as solid lines, *i.e.* the line in Fig. 1(a) indicates the heavy quark potential from Refs. [1, 27], and in Fig. 1(b) it indicates the zero level. As both, the internal energy and entropy, have been calculated using renormalized free energies proper renormalization of both observables is already incorporated by construction. It can clearly be deduced from Fig. 1(a) that the singlet free and internal energies smoothly approach $V(r)$ at small distances and the free energy thus indeed is dominated by the energy contribution. In fact, the entropy contribution shown in Fig. 1(b) is quite small at small distances and indicates a vanishing entropy contribution in the limit $r \to 0$. Unfortunately we could not go to smaller distances to clearly demonstrate this behavior. Moreover, at small distances $U_1(r,T)$ and $TS_1(r,T)$ suffer from lattice artifacts which result from small distance lattice artifacts in the free energies. At intermediate and large distances, however, the free and internal energies shown in Fig. 1(a) deviate from each other and $TS_1(r,T)$ indeed plays an important role for the behavior of $F_1(r,T)$. At asymptotic large distances the internal energies and entropies approach temperature dependent constant values, *i.e.* $U_\infty(T) \equiv \lim_{r\to\infty} U_1(r,T)$ and $S_\infty(T) \equiv \lim_{r\to\infty} S_1(r,T)$ are finite for finite temperatures. These values are indicated by the arrows in Fig. 1 and, in particular, at finite temperature

$$U_\infty(T) \gtrsim F_\infty(T) \qquad (16)$$

is evident.

A similar behavior of $U_\infty(T)$ and $S_\infty(T)$ can be deduced from high temperature perturbation theory. To

---

[1] We assume here the existence of an energy, $V_{\mathcal{O}}(r)$, at $T = 0$ which corresponds to the expectation value of $\lim_{T\to 0}\langle\mathcal{O}_r^{(c)}\rangle$.

[2] Details on our lattice simulations, in particular, on the calculation of $F_1(r,T)$, are given in Ref. [1]. Details on the computation of $U_1(r,T)$ and $S_1(r,T)$ will be given in Sec. III and IV.
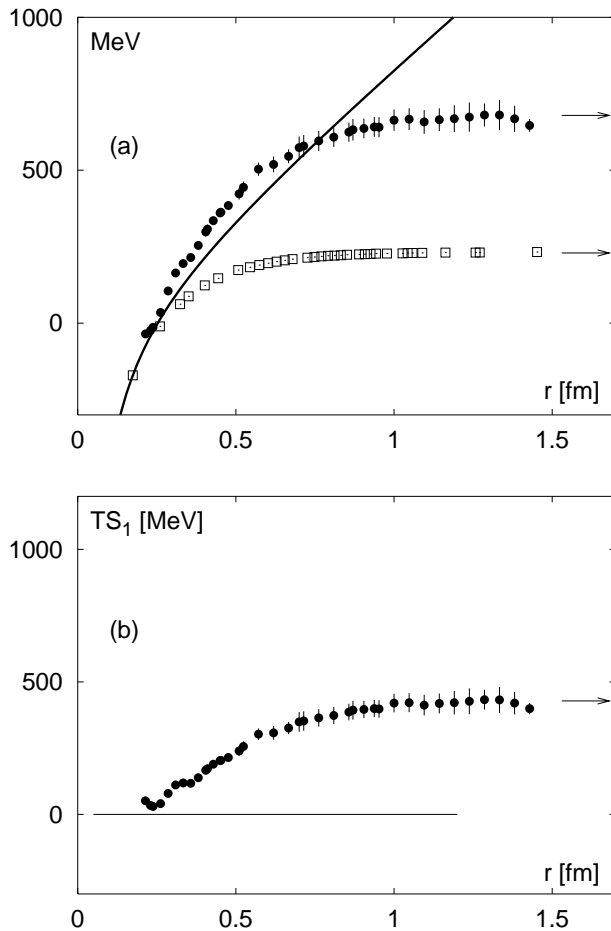
FIG. 1: (a) The singlet internal energy, $U_1(r,T)$ (filled circles), calculated from renormalized singlet free energy, $F_1(r,T)$ (open squares), at fixed $T \simeq 1.3T_c$ calculated in 2-flavor lattice QCD and compared them to $V(r)$ (line) [1, 27]. (b) The corresponding color singlet quark anti-quark entropy, $TS_1(r, T \simeq 1.3T_c)$, as function of distance calculated from renormalized free energies. The arrows point in both figures at the temperature dependent values of the free and internal energy and entropy at asymptotic large distances, i.e. $F_\infty(T) \equiv \lim_{r\to\infty} F_1(r,T)$, $U_\infty(T) \equiv \lim_{r\to\infty} U_1(r,T)$ and $TS_\infty(T) \equiv T \lim_{r\to\infty} S_1(r,T)$.

be more precise, high temperature perturbation theory suggests a cubic leading order dependence[3] of the free energy on the coupling [40], i.e.

$$F_\infty(T) \simeq -\frac{4}{3}m_D(T)\alpha(T) \simeq -\mathcal{O}(g^3 T) . \quad (17)$$

Here $\alpha(T) = g^2(T)/4\pi$ and $m_D(T)$ denotes the Debye

---

[3] Here and in what follows we already have anticipated the running of the coupling with the expected dominant scale T. Of course, the running of the coupling appears only beyond leading order.

---

mass which in re-summed leading order is given by

$$m_D(T) = \left(1+\frac{N_f}{6}\right)^{1/2} g(T)T . \quad (18)$$

We note that this leading order result is gauge invariant. In the following we use the renormalization group β-function to evaluate the derivatives of the coupling, i.e. for an arbitrary function $\mathcal{F} \equiv \mathcal{F}(g,T)$ we use

$$T\frac{d\mathcal{F}(g,T)}{dT} = T\frac{\partial\mathcal{F}(g,T)}{\partial T} + \beta(g)\frac{d\mathcal{F}(g,T)}{dg} , \quad (19)$$

where $\beta(g) = -\beta_0 g^3 + \mathcal{O}(g^5)$ in perturbation theory. Assuming this behavior the internal energy, $U_\infty(T)$, and entropy, $S_\infty(T)$, are expected to behave like

$$U_\infty(T) \simeq 4m_D(T)\alpha(T)\frac{\beta(g)}{g(T)} \simeq -\mathcal{O}(Tg^5) , \quad (20)$$

and

$$S_\infty(T) \simeq +\frac{4}{3}\frac{m_D(T)}{T}\alpha(T) + 4\frac{m_D(T)}{T}\alpha(T)\frac{\beta(g)}{g(T)}$$
$$\simeq +\mathcal{O}(g^3) . \quad (21)$$

The leading contribution to $TS_\infty(T)$ is similar to the free energy in Eq. (17) and thus at high temperatures and large distances the free energy is indeed expected to be to large extent dominated by the entropy contribution, i.e. at leading order $S_\infty(T) \simeq -F_\infty(T)/T$. Although the entropy itself will vanish logarithmically in the high temperature limit, i.e. $S_\infty(T \to \infty) = 0$, the contribution $TS_\infty(T)$ will clearly dominate the differences between free and internal energy at high temperatures,

$$U_\infty(T) - F_\infty(T) = TS_\infty(T) \simeq +\mathcal{O}(g^3 T) . \quad (22)$$

Thus, the difference between free and internal energy is expected to increase continuously with increasing temperature when approaching the perturbative high temperature regime. Only in the limit of zero temperature, $T \to 0$, the observable $TS_\infty(T)$ will vanish as $S_\infty(T)$ is a dimension less quantity which due to string breaking stays finite in QCD. Any qualitative change in the observable $TS_\infty(T)$ as function of temperature between both limits, i.e. $T \to 0$ and $T \to \infty$, is not quite obvious and, if present, may signal the phase change from the chiral symmetry broken phase at low to the deconfinement phase at high temperatures.

We may finally note that although we discuss in the following the internal energies and entropies calculated from renormalized free energies, it is conceptually quite satisfying that both observables could equally well be renormalized by matching their short distance parts to the heavy quark potential (14) and zero (15), respectively. This is indeed evident from Figs. 1(a, b). As no additional divergences get introduced at finite temperature also their large distance properties are properly fixed in the continuum limit, in particular, also the manifestly gauge invariant observables $U_\infty(T)$ and $S_\infty(T)$.

T/T_c	S_∞	U_∞/T_c
0.79	5.48 (259)	9.37 (207)
0.84	6.49 (119)	10.19 (101)
0.88	7.78 (168)	11.30 (148)
0.93	12.92 (138)	15.96 (129)
0.98	16.38 (113)	19.27 (112)
1.01	14.83 (172)	17.71 (173)
1.04	12.93 (825)	15.78 (88)
1.09	5.49 (42)	7.84 (46)
1.13	3.95 (41)	6.14 (46)
1.19	2.73 (25)	4.72 (29)
1.29	1.63 (16)	3.37 (21)
1.43	1.25 (11)	2.85 (16)
1.57	1.02 (8)	2.51 (12)
1.72	0.91 (10)	2.32 (17)
1.89	0.87 (7)	2.26 (14)
2.99	0.67 (1)	2.09 (2)

TABLE I: The change in internal energy and entropy due to the presence of a quark anti-quark pair at infinite separation in the QCD heat bath versus temperature.

III. THE CONFINEMENT DECONFINEMENT TRANSITION

We begin our discussion of the finite temperature energies and entropies at asymptotic large distances, $r \rightarrow \infty$. Actually, to avoid any fit we again [1] approximated the value of the free energy at infinite distance, $F_1(r \rightarrow \infty, T)$, by the value of the quark anti-quark free energy calculated at the largest possible separation on the lattice, i.e. $F_\infty(T) \equiv F_{\bar{q}q}(N_\sigma/2, T)$, and calculated separately the internal energy, $U_\infty(T)$, and entropy, $S_\infty(T)$. Both quantities are obtained from derivatives of the color averaged free energy, $F_{\bar{q}q}(r, T)$, which is a manifestly gauge invariant observable. Our results for $U_\infty(T)$ and $S_\infty(T)$ are summarized in Tab. I. It is quite satisfying that the values obtained for $U_\infty(T)$ and $S_\infty(T)$ reproduce the free energy given in Tab. 2 of Ref. [1], i.e. the quantity $U_\infty - TS_\infty$ matches to the value for $F_\infty = -2T \ln |\langle L \rangle|$ for all temperatures.

In parts of our analysis we are also interested in the flavor and quark mass dependence of the finite temperature energies and entropies. We thus again [1] compare our results ($N_f = 2$) to results from quenched QCD ($N_f = 0$) [5, 41] and also in parts to a recent study of 3-flavor QCD [26]. To convert the observables to physical units we use $T_c = 270$ MeV in quenched, $T_c = 200$ MeV in 2-flavor ($m_\pi/m_\rho \simeq 0.7$) and $T_c = 193$ MeV in 3-flavor ($m_\pi/m_\rho \simeq 0.4$) QCD. It should be obvious, however, that a comparison of free and internal energies crucially depends on the relative normalization of the corresponding zero temperature heavy quark potentials used for renormalization and thus a comparison could be affected by flavor and/or quark mass dependent (over-all)

constant contributions. Here, and in what follows, the relative normalization of the heavy quark potentials in quenched and full QCD is such that there is no constant contribution in the Cornell Ansatz for $V(r)$ at large distances. We also note that any undetermined constant contribution to the heavy quark potential at zero temperature will add a non-perturbative over-all constant to the free and internal energies which would also affect the comparison of these observables with perturbation theory [42]. We stress again, however, that the quark anti-quark entropy is unaffected by any undetermined finite renormalization of $V(r)$ at zero temperature, i.e. $S_\infty(T)$ does not dependent on any flavor and/or quark mass dependent normalization terms that could contribute to $V(r)$ at $T = 0$.

A. The free energy

Our results for $F_\infty(T)$ are summarized in Fig. 2 as function of T/T_c and compared to $F_\infty(T)$ obtained in quenched and 3-flavor QCD. While $F_\infty(T)$ in quenched QCD exhibits a singularity at T_c due to the first order phase transition and is infinite below T_c, it is well-defined and finite in full QCD at all temperatures due to string breaking below and color screening above the transition. In this case $F_\infty(T)$ is steadily decreasing with increasing temperatures in the whole temperature range analyzed
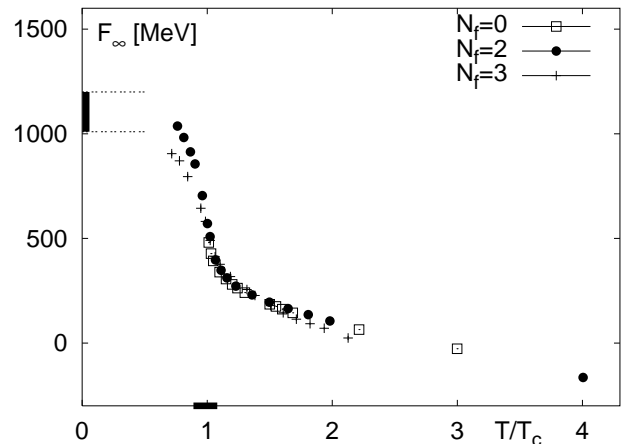

FIG. 2: The value of the free energies $F_\infty(T)$ at asymptotic large distances as function of temperature in physical units. We compare here our results from 2-flavor QCD ($T_c = 200$ MeV, $m_\pi/m_\rho \simeq 0.7$) to the results in pure gauge theory ($T_c = 270$ MeV) [5] and 3-flavor QCD ($T_c = 193$ MeV, $m_\pi/m_\rho \simeq 0.4$) [26]. The dashed horizontal lines show the expected energy $V(r_{\text{breaking}}) \simeq 1000 \sim 1200$ fm using $r_{\text{breaking}} \simeq 1.2 - 1.4$ fm from 2-flavor lattice studies at $T = 0$ and quark mass $m_\pi/m_\rho \simeq 0.7$ [43]. In 2-flavor lattice studies at $T = 0$ and lower quark mass, $m_\pi/m_\rho \simeq 0.4$, the string is expected to break at smaller (lower) distances (energies) [44]. The thick line around T_c is explained in Sec. III B.
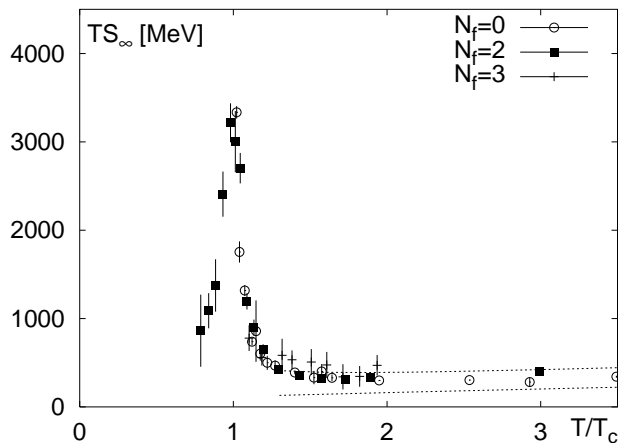
FIG. 3: The contribution $TS_\infty(T)$ appearing in the free energy, $F_\infty(T) = U_\infty(T) - TS_\infty(T)$, calculated in 2-flavor QCD as function of T/T_c. We compare our results from 2-flavor QCD to the leading order part of Eq. (21) (or Eq. (22)) using the 2-loop formula for the coupling (23) with $T_c/\Lambda_{\overline{MS}} = 0.77(15)$ [21, 45] and scales $\mu = \pi, ..., 4\pi$ (dashed lines). We also show results from 3-flavor QCD for $T \gtrsim 1.1T_c$ [26] and quenched QCD [5, 41, 46].

by us. A discussion of $F_\infty(T)$, in particular for $T \lesssim T_c$, has already been given [1, 28]. We may add here that the slope of $F_\infty(T)$ as function of temperature indeed turns out to be maximal in the vicinity of the transition. Although flavor and/or quark mass dependences of the observable $F_\infty(T)$ can clearly be seen when comparing the data for 2- and 3-flavor QCD, at temperatures about $1.2T_c \lesssim T \lesssim 2T_c$ no or only little differences between quenched and full QCD could be identified. Flavor dependences are, however, to be expected when reaching temperatures in the perturbative regime.

B. The entropy

The entropy contribution, $TS_\infty(T)$, obtained in 2-flavor QCD is shown in Fig. 3 as function of T/T_c and is again compared to results from quenched and 3-flavor QCD. We indeed find $TS_\infty(T) \geq 0$ at all temperatures analyzed here. Moreover, the data for $TS_\infty(T)$ at low temperatures also suggest a vanishing contribution in the zero temperature limit, $T \to 0$. Unfortunately we could not go to smaller temperatures to clearly demonstrate this behavior. On the other hand, in the high temperature phase, i.e. at $T \gtrsim 2T_c$, we indeed find a tendency for an increase of $TS_\infty(T)$ with temperature as expected from (22). Actually, this small increase is consistent with the rise given in (21). To demonstrate this we also compared $TS_\infty(T)$ in 2-flavor QCD to Eq. (21) using the

perturbative 2-loop coupling, i.e.

$$g_{2-loop}^{-2}(T) = 2\beta_0 \ln\left(\frac{\mu T}{\Lambda_{\overline{MS}}}\right) + \frac{\beta_1}{\beta_0} \ln\left(2\ln\left(\frac{\mu T}{\Lambda_{\overline{MS}}}\right)\right), \tag{23}$$

with

$$\beta_0 = \frac{1}{16\pi^2}\left(11 - \frac{2N_f}{3}\right),$$

$$\beta_1 = \frac{1}{(16\pi^2)^2}\left(102 - \frac{38N_f}{3}\right),$$

assuming vanishing quark masses. We used $T_c/\Lambda_{\overline{MS}} = 0.77(15)$ [21, 45, 47] and the ambiguity in fixing the scale in perturbation theory, $\mu = \pi, ..., 4\pi$. This estimate is shown within the dashed lines and qualitatively agrees with the lattice data for $T \gtrsim 2T_c$. However, to clearly establish the perturbative increase of $TS_\infty(T)$ with increasing temperature will require the analysis of significantly higher temperatures. We also note that within the statistical accuracy of the data we find for $T \gtrsim 2T_c$ the tendency,

$$S_\infty^{N_f=0}(T) \lesssim S_\infty^{N_f=2}(T) \lesssim S_\infty^{N_f=3}(T). \tag{24}$$

It appears indeed quite reasonable that introducing additional flavor degrees of freedom may enhance the finite temperature quark anti-quark entropy in the deconfined phase. It is, however, quite difficult to separate clearly the different effects from flavor and quark mass dependence in full QCD. In particular, at temperatures below T_c the tendency given in (24) may change as can be seen from the temperature dependence of $F_\infty(T)$ shown in Fig. 2.

In contrast to the small temperature dependence of $TS_\infty(T)$ at low and high temperatures, $TS_\infty(T)$ shows qualitatively and quantitatively significant differences at temperatures in the vicinity of the transition. In fact, $TS_\infty(T)$ obtained in 2-flavor QCD exhibits a sharp peak at T_c. This behavior signals the high temperature phase transition/crossover in QCD. As the peak is so sharp we may introduce T_l (T_u) defined as the lower (upper) temperature at which $S_\infty(T)$ approaches about half of the peak value, i.e. $S_\infty(T_{l,u}) \equiv S_\infty(T_c)/2$. We find for 2-flavor QCD T_l about $0.89T_c$ and T_u about $1.07T_c$ using $S_\infty(T_c) \simeq 16.5$. This temperature range is shown at the bottom of Fig. 2 as thick line. A similar behavior is also apparent in 3-flavor QCD. This indicates that the crossover from the low to the high temperature phase in QCD takes place in a small temperature range around T_c. We stress, however, that the temperature dependence of $F_\infty(T)$ also at temperatures above $1.07T_c$ is still to a large extent dominated by non-perturbative effects.

C. The internal energy

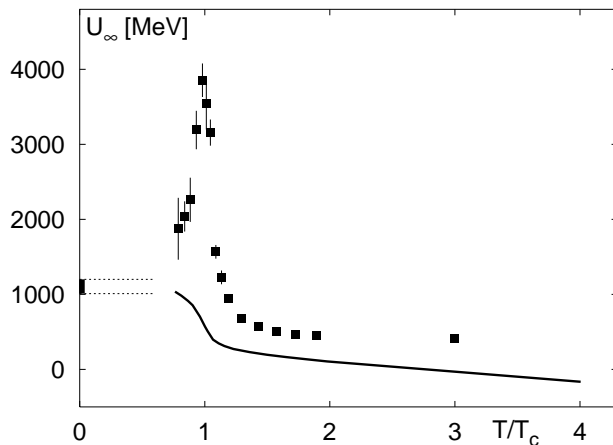The internal energy, $U_\infty(T)$, in 2-flavor QCD is shown in Fig. 4 as function of temperature and is compared

FIG. 4: The internal energy $U_\infty(T)$ versus T/T_c calculated in 2-flavor QCD. The corresponding free energy, $F_\infty(T)$, calculated in 2-flavor QCD is also shown as solid line. We again indicate in this figure the energy at which string breaking is expected to take place at $T = 0$, $V(r_{\text{breaking}}) \simeq 1000 - 1200$ MeV (dashed lines), using $r_{\text{breaking}} = 1.2 - 1.4$ fm [43].

to the corresponding free energy, $F_\infty(T)$ (solid line), already shown in Fig. 2. We indeed find $U_\infty(T) > F_\infty(T)$ at all temperatures analyzed here. It can clearly be seen that the temperature dependence of $F_\infty(T)$ and $U_\infty(T)$ is qualitatively and quantitatively different. While the free energy steadily decreases with increasing temperatures the internal energy exhibits a pronounced peak. Again this peak is sharply localized at the (pseudo-) critical temperature. At the temperatures analyzed by us the internal energy below T_c is rapidly increasing with increasing temperatures. Again we indicate by dotted lines the plateau value of the heavy quark potential at zero temperature, $V(r_{\text{breaking}}) \simeq 1000 - 1200$ MeV, using $r_{\text{breaking}} \simeq 1.2 - 1.4$ fm [43]. A comparison of $U_\infty(T)$ with this value shows again that most of the temperature dependence of $U_\infty(T)$ is sharply localized at temperatures in the vicinity of the transition. A qualitatively similar behavior is also apparent in 3-flavor QCD [26]. Comparing the available data some flavor or quark mass dependence, $U_\infty^{N_f=2}(T_c) \simeq 4000$ MeV $\gtrsim U_\infty^{N_f=3}(T_c) \simeq 3000$ MeV, can be observed and also the value $U_\infty(T_c^+)$ in quenched QCD [41] is of similar magnitude. As noted in Sec. II B, however, the values for $U_\infty(T)$ may depend on the relative normalization of $V(r)$ at $T = 0$ used for renormalization.

At temperatures above T_c, $U_\infty(T)$ rapidly drops while at higher temperatures, *i.e.* $T \gtrsim 1.3T_c$, the temperature dependence of $U_\infty(T)$ turns out to be much weaker than in the vicinity of phase transition. However, contact with the perturbative relation, Eq. (20), is not expected at those temperatures as $U_\infty(T)$ is still positive. In fact, when approaching the perturbative high temperature regime also $U_\infty(T)$ is expected to exhibit a change in sign and will slowly diverge with respect to (20).

IV. FINITE TEMPERATURE ENERGIES AND POTENTIAL MODELS

The analysis of bound state problems has been quite successful in terms of potential theory at $T = 0$ [48, 49, 50]. For the discussion of quarkonium suppression patterns at finite temperature one also often resorts to potential models [9, 11, 13, 14, 17]. Of course, the strong interaction remains unaffected by temperature and the modeling of thermal modifications of heavy quark bound states requires the definition of an effective potential, $V_{\text{eff}}(r, T)$ [2], which can be given only phenomenologically, for instance, by using the modifications of the free and internal energies. It is thus important to understand the binding properties of the different finite temperature energies. For this purpose we also calculated the quark anti-quark internal energies for the temperatures given in Tab. I at several finite distances. Parts of our results for $U_1(r, T)$ are summarized in Fig. 5 at temperatures below (a) and above (b) the transition. Similar results have been obtained for internal energies in the averaged and octet channels.

To gain some insight into the consequences these energies have for quarkonium dissociation we compare the asymptotic ($r \to \infty$) energies with the potential energies at a distance corresponding to the size of some quarkonium states,

$$\Delta E_i(T = 0) \equiv V(\infty) - V(r_i) , \qquad (25)$$

where the radii r_i ($i = J/\psi, \chi_c, ...$) are listed in the first row of Tab. II. At zero temperature $V(\infty)$ is taken to be twice the energy needed to create the lowest heavy-light meson. For our purpose we consider $V(\infty) \equiv V(r_{\text{breaking}}) \simeq 1000$ MeV where r_{breaking} is the distance at which the string is expected to break at zero temperature, $r_{\text{breaking}} \gtrsim 1.2$ fm [43]. This energy is shown in Fig. 6 as horizontal line. The resulting energy for J/ψ is also shown. The energies for some charmonium and bottomonium states are summarized in Tab. II and compared to the mass difference obtained from $2M_{D,B} - m_i$ where $M_{D,B}$ denotes the D- and B-meson masses and m_i the masses of the different quarkonium states [51]. Of course, the wave functions for the different quarkonium states will also reach out to larger distances [50] and thus our estimate for the different energy levels $E_i(T = 0)$ can only be taken as indicative for the relevant energies. Potential model analysis, using for instance the Schrödinger equation, will do better in this respect.

Similarly we can estimate the temperature dependence of the energy levels for the different quarkonium states from $E_i(T) \equiv V_{\text{eff}}(r_i, T)$. Again these energy levels will only characterize the relevant energies and the sizes of these states may also become temperature dependent. At finite temperature, however, the values for these levels are expected to depend crucially also on the specific modeling of the effective potential, $V_{\text{eff}}(r, T)$. This is obvious from the different energy levels for the J/ψ shown in

state	J/ψ	χ_c	$\psi\prime$	Υ	χ_b	$\Upsilon\prime$
r_i [fm]	0.45	0.70	0.87	0.23	0.41	0.51
$2M_{D,B} - m_i$ [MeV]	631	313	42	1098	698	535
$\Delta E_i(T=0)$ [MeV]	830	560	400	1140	870	750
$\Delta E_i(T_c)$ [MeV] [using F_1]	321	124	62	665	334	265
$\Delta E_i(T_c)$ [MeV] [using U_1]	3036	1618	1010	3721	3085	2615
$\Delta E_i(T_c)$ [MeV] [using $F_{\bar{q}q}$]	97	27	12	607	87	55
$\Delta E_i(T_c)$ [MeV] [using $U_{\bar{q}q}$]	1355	747	504	3732	1392	1136
$T_{\rm dis}^{\rm PM}/T_c$ [potential model using F_1]	1.1	0.74	0.1 - 0.2	2.31	1.13	1.1
$T_{\rm dis}^{\rm PM}/T_c$ [potential model using U_1]	~ 2	~ 1.1	~ 1.1	~ 4.5	~ 2	~ 2
$T_{\rm dis}^{\rm SF}$ from lattice spectral functions	$1.5 - 3$	$\lesssim 1.1$				

TABLE II: A summary of the different estimates for the relevant temperatures, $T_{\rm dis}$, at which quarkonium dissociation is expected to become important. In the first row we give the mean squared charge radii, r_i, and the energies, $\Delta E_i(T=0) \equiv V(\infty) - V(r_i)$ at zero temperature with $V(\infty) \simeq 1000$ MeV. We also list the mass gap $2M_{D,B} - m_i$ using D- and B-meson masses $M_D = 1864$ MeV and $M_B = 5279$ MeV, respectively [51]. The second row summarizes results for the break up energies at T_c estimated from $\Delta E_i(T_c) \equiv V_{\rm eff}(r_i, T_c) - V_{\rm eff}(\infty, T_c)$ using different definitions for $V_{\rm eff}(r,T)$. The errors on these values are typically about 20%. Note here that the thermal energy $E_{th}(T) = 3T$ is about 600 MeV at T_c. The 3$^{\rm rd}$ and 4$^{\rm th}$ row contain different values for the relevant dissociation temperatures, *i.e.* estimates for the onset of temperature effects in quarkonium states, $T_{\rm onset}$ [1, 2], the predicted dissociation temperatures from potential model calculations ($T_{\rm dis}^{PM}$) [9, 13, 14], and lattice studies of charmonium spectral functions, $T_{\rm dis}^{\rm SF}$ [52, 53].

Fig. 6 which we obtained by using as $V_{\rm eff}(r,T)$ the singlet free energy (lower dashed line) and singlet internal energy (upper dashed line). Due to the steeper rise of the internal energy compared to free energy $E_{J/\psi}(T)$ is enhanced compared to the energy level obtained from the internal energy. It is interesting to note here that $E_{J/\psi}(T = 1.3T_c)$ deduced from the internal energy is even larger than at zero temperature while in terms of the free energy it is smaller than $E_{J/\psi}(T=0)$. For the characterization of the relevant energies needed to dissociate the bound state we again consider $\Delta E_i(T) \equiv V_{\rm eff}(\infty, T) - V_{\rm eff}(r_i, T)$, which depends on the definition of $V_{\rm eff}(r,T)$. This is evident from Fig. 7 where we show the temperature dependence of $\Delta E_{J/\psi}(T)$ estimated from $V_{\rm eff}(r,T) \equiv U_1(r,T)$ (filled circles) and $V_{\rm eff}(r,T) \equiv F_1(r,T)$ (open circles). While $\Delta E_{J/\psi}(T)$ is continuously decreasing with increasing temperatures when using $F_1(r,T)$ as effective potential, its binding pattern appears quite different from what one obtains by using $V_{\rm eff}(r,T) \equiv U_1(r,T)$. Actually, in the latter case the binding pattern exhibits a maximum in the vicinity of the transition while it rapidly drops above T_c. Similar results have been obtained also for other charmonium and bottomonium states and are summarized in Tab. II.

Of course, the model dependences of the dissociation energies at finite temperature also affect the analysis of suppression patterns and corresponding dissociation temperatures [9, 13, 14]. Actually, using $V_{\rm eff}(r,T) \equiv U_1(r,T)$ suggests that suppression of J/ψ may occur only at temperatures close but above the transition while from $V_{\rm eff}(r,T) \equiv F_1(r,T)$ one finds that J/ψ dissolves already at temperatures below the crossover. Similar model dependences enter also the analysis of excited quarkonium states and the corresponding estimates for the dissocia-

tion temperatures are summarized in Tab. II using four different definitions for $V_{\rm eff}(r,T)$, *i.e.* we used the singlet free and internal energies ($F_1(r,T)$, $U_1(r,T)$) as well as the finite temperature energies in the color averaged channel ($F_{\bar{q}q}(r,T)$, $U_{\bar{q}q}(r,T)$).

V. SUMMARY AND CONCLUSIONS

Following [5, 6] we introduced and analyzed the change in internal energy and entropy due to the presence of a static quark anti-quark pair in a QCD heat bath. Both observables are introduced as intensive observables as appropriate derivatives of the renormalized free energy. Similar to the singlet quark anti-quark free energies [1, 5, 42, 54] also the singlet internal energies become temperature independent in the limit of small distances and are controlled by the zero temperature running coupling.

We analyzed qualitative and quantitative differences that appear when changing from free energies to internal energies as observable that defines an effective potential that can be used in model calculations. We discussed the important role of the entropy contribution at finite temperature. At short distances, at intermediate and at large distances the entropy contribution is non-zero and shows non-trivial r-dependences. We find positive entropy contributions, $S_1(r,T) \gtrsim 0$, and thus $U_1(r,T) \gtrsim F_1(r,T)$. Similar to the free energies, also the large distance properties of the internal energies and entropies are controlled by string breaking below and color screening above deconfinement and both approach temperature dependent constant values, which define $U_\infty(T)$ and $S_\infty(T)$, at asymptotic large distances.
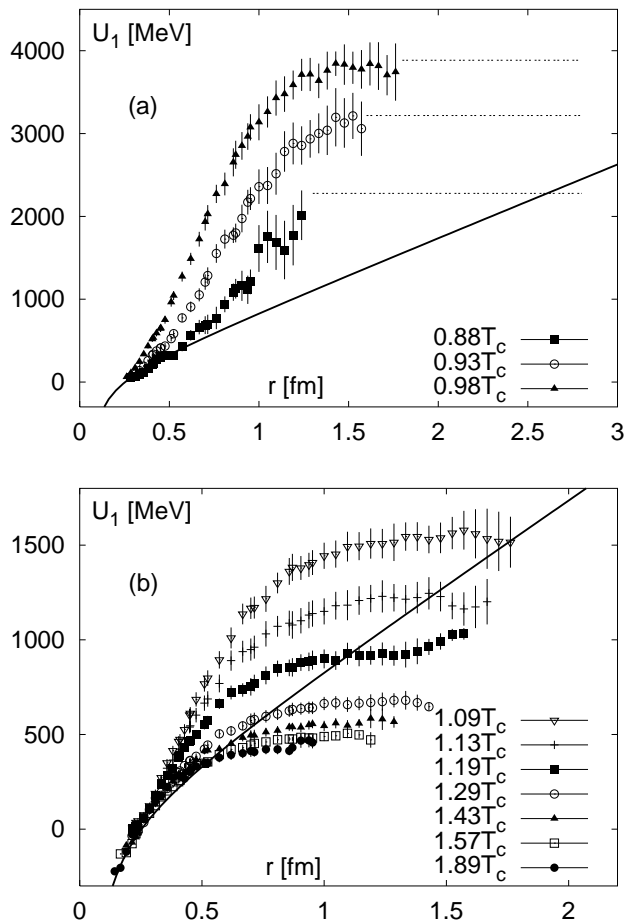
FIG. 5: The color singlet quark anti-quark internal energies, $U_1(r,T)$, at several temperatures below (a) and above (b) the phase transition obtained in 2-flavor lattice QCD. In (a) we also show as horizontal lines the asymptotic values given in Tab. I which are approached at large distances and indicate the flattening of $U_1(r,T)$. The solid lines represent in each figure the $T=0$ heavy quark potential, $V(r)$ [1, 27].

Actually, the difference between free and internal energies at high temperatures, $TS_\infty(T) \simeq 4m_D(T)\alpha(T)/3$, is supposed to increase with increasing temperatures. In particular, $U_\infty(T)$ and $S_\infty(T)$, are, similar to $F_\infty(T)$ [5], again introduced as manifest gauge invariant observables and clearly signal the QCD plasma transition. In fact, while the plateau values which are approached by the free energies, $F_\infty(T)$, are rapidly decreasing in the vicinity of the transition [1, 28], the values approached by the internal energies, $U_\infty(T)$, and entropies, $S_\infty(T)$, show both a sharp peak at the (pseudo-) critical temperature. Similar results are also obtained in quenched and 3-flavor QCD [5, 6, 26, 41]. However, qualitative differences become quite transparent in the vicinity and below the transition when comparing these observables obtained in quenched and full QCD. In quenched QCD the first order phase transition is related to singularities in thermodynamic

observables which can indeed be seen after renormalization in the temperature dependence of the finite temperature energies, entropies and the renormalized Polyakov loop (see also [1, 5, 46]). In contrast to quenched QCD, in full QCD the phase change is a crossover and we consequently do not see any singularities in the finite temperature energies and entropies nor in the temperature dependence of the renormalized Polyakov loop [1].

We also investigated the temperature dependence of quarkonium binding in the vicinity of the transition. For this purpose we used the finite temperature energies to define appropriate effective potentials, $V_{\rm eff}(r,T)$, as one would do in potential models. As effective potentials we used the singlet and averaged free and internal energies, i.e. we defined $V_{\rm eff}(r,T)$ through $F_1(r,T)$, $F_{\bar{q}q}(r,T)$, $U_1(r,T)$ and $U_{\bar{q}q}(r,T)$, and estimated the binding energies at temperatures below and above the transition. In all cases the binding energies of the quarkonium states indeed become weaker with increasing temperatures above the transition and this may lead to dissociation of parts of these states at temperatures close but above T_c. Our analysis, however, shows strong dependencies of the binding energies and dissociation temperatures on the specific modeling of $V_{\rm eff}(r,T)$. To some extent these model dependencies enter from quite general grounds when exchanging the definition of $V_{\rm eff}(r,T)$ from free energies into internal energies. When using free energies the binding energies continuously and rapidly decrease when crossing the transition and most of the quarkonium bound states
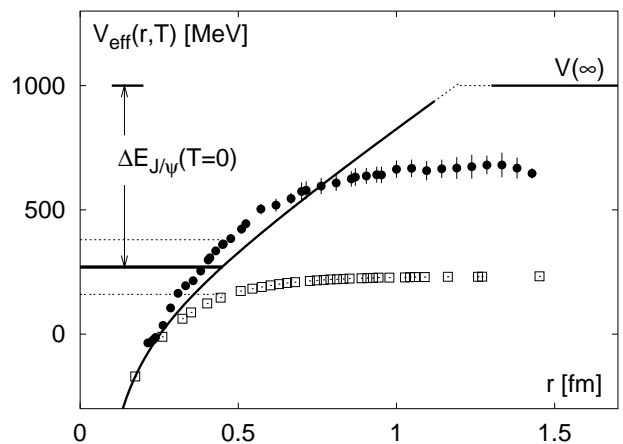

FIG. 6: Different effective potentials in the color singlet channel, $V_{\rm eff}(r,T) \equiv F_1(r,T)$ (open symbols) and $V_{\rm eff}(r,T) \equiv U_1(r,T)$ (filled symbols), at fixed $T \simeq 1.3T_c$ as function of distance and the heavy quark potential, $V(r)$. We also compare $V_{\rm eff}(r,T)$ to the J/ψ energy level at $T=0$, $E_{J/\psi}(T=0) \equiv V(r=r_{J/\psi}) \simeq 270$ MeV (horizontal solid line). The horizontal dashed lines correspond to the J/ψ energy levels defined on $E_{J/\psi}(F_1) \equiv F_1(r_{J/\psi},T)$ (lower dashed line) and $E_{J/\psi}(U_1) \equiv U_1(r_{J/\psi},T)$ (upper dashed line). $r_{J/\psi} \simeq 0.45$ fm is fixed through the mean squared charge radius expected at $T=0$ given in Tab. II.
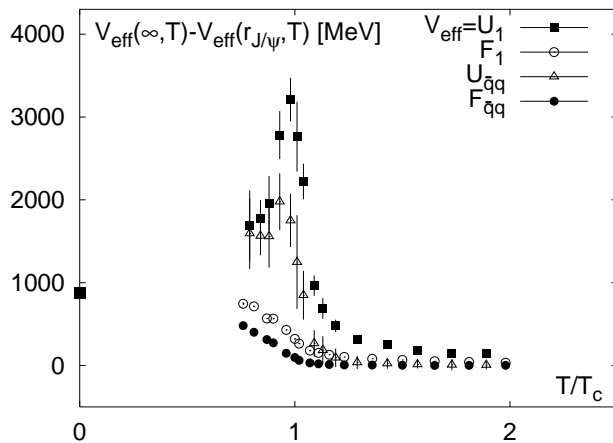
FIG. 7: The energy difference $V_{\text{eff}}(\infty, T) - V_{\text{eff}}(r_{J/\psi}, T)$ as function of temperature using the different energies as effective potential, $V_{\text{eff}}(r, T) \equiv U_1(r, T)$, $F_1(r, T)$, $U_{\bar{q}q}(r, T)$, $F_{\bar{q}q}(r, T)$.

may thus indeed dissolve at temperatures in the vicinity and below the transition [13, 14]. The temperature dependence of the binding energies deduced from internal energies, however, turns out to be more complicated in the vicinity of the transition. An effective potential defined through quark anti-quark internal energies suggests increasing binding energies below the transition which exhibit a peak at T_c. This may imply that all quarkonium states analyzed here are still bound at the transition. The binding energies of the different states rapidly decrease above T_c leading again to quarkonium dissociation, however, the temperatures which are relevant for dissociation are shifted to larger temperatures than those deduced from free energies. The recent potential model calculations [9, 10] using the properties of $U_1(r, T)$ at temperatures above the transition as well as the lattice analysis of quarkonium bound states in quenched QCD [52, 53] support our findings.

Acknowledgments

[1] O. Kaczmarek and F. Zantow, hep-lat/0503017.
[2] F. Karsch, hep-lat/0502014.
[3] L. D. McLerran and B. Svetitsky, Phys. Rev. **D24**, 450 (1981).
[4] L. D. McLerran and B. Svetitsky, Phys. Lett. **B98**, 195 (1981).
[5] O. Kaczmarek, F. Karsch, P. Petreczky, and F. Zantow, Phys. Lett. **B543**, 41 (2002).
[6] F. Zantow, O. Kaczmarek, F. Karsch, and P. Petreczky, hep-lat/0301015.
[7] T. Matsui and H. Satz, Phys. Lett. **B178**, 416 (1986).
[8] G. E. Brown, C.-H. Lee, and M. Rho, Nucl. Phys. **A747**, 530 (2005).
[9] C.-Y. Wong, hep-ph/0408020.
[10] E. V. Shuryak and I. Zahed, Phys. Rev. **D70**, 054507 (2004).
[11] H.-J. Park, C.-H. Lee, and G. E. Brown, hep-ph/0503016.
[12] N. Brambilla *et al.*, hep-ph/0412158.
[13] S. Digal, P. Petreczky, and H. Satz, Phys. Lett. **B514**, 57 (2001).
[14] S. Digal, P. Petreczky, and H. Satz, Phys. Rev. **D64**, 094015 (2001).
[15] C.-Y. Wong, J. Phys. **G28**, 2349 (2002).
[16] C.-Y. Wong, Phys. Rev. **C65**, 034902 (2002).
[17] E. V. Shuryak and I. Zahed, Phys. Rev. **C70**, 021901 (2004).
[18] O. Kaczmarek, F. Karsch, E. Laermann, and M. Lutgemeier, Phys. Rev. **D62**, 034021 (2000).
[19] O. Kaczmarek, F. Karsch, F. Zantow, and P. Petreczky, Phys. Rev. **D70**, 074505 (2004).
[20] B. Beinlich, F. Karsch, E. Laermann, and A. Peikert, Eur. Phys. J. **C6**, 133 (1999).
[21] F. Karsch, E. Laermann, and A. Peikert, Phys. Lett. **B478**, 447 (2000).
[22] R. D. Pisarski, hep-ph/0203271.
[23] O. Kaczmarek, S. Ejiri, F. Karsch, E. Laermann, and F. Zantow, Prog. Theor. Phys. Suppl. **153**, 287 (2004).
[24] A. Dumitru, Y. Hatta, J. Lenaghan, K. Orginos, and R. D. Pisarski, Phys. Rev. **D70**, 034511 (2004).
[25] A. Dumitru, J. Lenaghan, and R. D. Pisarski, Phys. Rev. **D71**, 074004 (2005).
[26] P. Petreczky and K. Petrov, Phys. Rev. **D70**, 054503 (2004).
[27] O. Kaczmarek and F. Zantow, hep-lat/0502012.
[28] O. Kaczmarek and F. Zantow, hep-lat/0502011.
[29] For a review of this subject and further references see [22]. For a non-perturbative lattice renormalization of Polyakov loop correlation functions see Refs. [1, 5, 42].
[30] S. Nadkarni, Phys. Rev. **D34**, 3904 (1986).
[31] O. Philipsen, Phys. Lett. **B535**, 138 (2002).
[32] N. Attig, F. Karsch, B. Petersson, H. Satz, and M. Wolff, Phys. Lett. **B209**, 65 (1988).
[33] O. Kaczmarek, F. Karsch, P. Petreczky, and F. Zantow, Nucl. Phys. Proc. Suppl. **129**, 560 (2004).
[34] A. Nakamura and T. Saito, Prog. Theor. Phys. **111**, 733 (2004).
[35] G. Boyd *et al.*, Nucl. Phys. **B469**, 419 (1996).
[36] G. Boyd *et al.*, Phys. Rev. Lett. **75**, 4169 (1995).

[37] I. Montvay and G. Munster, Cambridge Univ. Press (1994).

[38] L. S. Brown and W. I. Weisberger, Phys. Rev. **D20**, 3239 (1979).

[39] S. Nadkarni, Phys. Rev. **D33**, 3738 (1986).

[40] E. Gava and R. Jengo, Phys. Lett. **B105**, 285 (1981).

[41] F. Zantow, Ph.D. thesis, Bielefeld University, Germany (2004).

[42] F. Zantow, hep-lat/0301014.

[43] P. Pennanen and C. Michael, hep-lat/0001015.

[44] C. W. Bernard *et al.*, Phys. Rev. **D64**, 074509 (2001).

[45] M. Gockeler *et al.*, hep-ph/0502212.

[46] O. Kaczmarek, P. Petreczky, and F. Zantow, to be published .

[47] M. Laine and Y. Schroder, JHEP **03**, 067 (2005).

[48] E. Eichten, K. Gottfried, T. Kinoshita, K. D. Lane, and T.-M. Yan, Phys. Rev. **D17**, 3090 (1978).

[49] E. Eichten, K. Gottfried, T. Kinoshita, K. D. Lane, and T.-M. Yan, Phys. Rev. **D21**, 203 (1980).

[50] S. Jacobs, M. G. Olsson, and C. J. Suchyta, Phys. Rev. **D33**, 3338 (1986).

[51] Particle Data Group, S. Eidelman *et al.*, Phys. Lett. **B592**, 1 (2004).

[52] M. Asakawa and T. Hatsuda, Phys. Rev. Lett. **92**, 012001 (2004).

[53] S. Datta, F. Karsch, P. Petreczky, and I. Wetzorke, Phys. Rev. **D69**, 094507 (2004).

[54] F. Zantow, O. Kaczmarek, F. Karsch, and P. Petreczky, Nucl. Phys. Proc. Suppl. **106**, 519 (2002).